

Dynamics of heteronuclear spin coupling and decoupling in solids

M. Mehring and G. Sinnig

Institut für Physik, University of Dortmund, 4600 Dortmund 50/Germany

(Received 27 September 1976)

In solids containing two nuclear-spin species I and S , the magnetic dipolar coupling causes exchange of order between and within the different spin subsystems. The dynamics involved are investigated theoretically by applying the memory-function approach. The experimentally observed line-broadening and line-narrowing effects in AgF and adamantane ($C_{10}H_{16}$) can be accounted for quantitatively by assuming a functional form for the memory function.

I. INTRODUCTION

Heteronuclear-spin coupling and decoupling in solids and its influence on the linewidth of the nuclear-magnetic-resonance (NMR) signal has been of considerable interest in the past.¹⁻⁵ A variety of NMR double-resonance experiments have been developed recently using the nuclear magnetic dipole-dipole interaction between abundant I spins and rare or weak S spins in order to detect the NMR spectrum of the S spins in solids.⁵⁻¹⁵ Magnetic dipolar interaction between I and S spins as represented by the Hamiltonian \mathcal{H}_{IS} causes an "inhomogeneous" broadening of the S -spin resonance line and supplies the coupling mechanism for polarization transfer from the I - to the S -spin subsystem and vice versa. Coupling and decoupling of both spin systems in the rotating frame is therefore achieved by rf fields applied close to the resonance frequency of the I and S spins, respectively. A "modulation" of the interaction results, i.e., \mathcal{H}_{IS} is rendered time dependent. In other words the effective interaction Hamiltonian can be manipulated at the experimenters will and the full dynamic range of the interactions involved can be studied.¹² We concentrate in this paper on the case, where a strong rf field $H_{II} = \omega_{1I}/\gamma_I$ is applied in a pulsed or continuous fashion close to the resonance frequency of the I spins. If the rf field is much stronger than the coupling of I and S spins ($\omega_{1I} \gg \|\mathcal{H}_{IS}\|$) and is applied at exact resonance of the I spins, a flipping of the I spins occurs, which is rapid compared with $\|\mathcal{H}_{IS}\|$. The time average of $\mathcal{H}_{IS}(t)$ vanishes and consequently the excess broadening of the S spin resonance line due to coupling to the I spins is zero.

To be more quantitative we ask how strong does ω_{1I} have to be in order to average out the heteronuclear coupling? At first sight it would appear that we require ω_{1I} large compared with $(M_2^{IS})^{1/2}$, where M_2^{IS} is the second moment of the S spins due to the I - S coupling. This would certainly be true,

if interactions among the I spins could be neglected. It is therefore no surprise, that this argument holds to a certain degree in some alkali halides,⁴ where $\gamma_I/\gamma_S \approx 1$. However, in the case $\gamma_I/\gamma_S \gg 1$ the flip-flop motion of the I spins, caused by the exchange term in their secular dipolar interaction, can appreciably modify the heteronuclear coupling of the two spin systems as was first shown by Abragam and Winter.^{1a,2} This flip-flop motion of the I spins competes with the rf field induced flipping of the I spins. The coherent motion imposed by the rf field can be destroyed by the flip-flop process between the I spins, reducing the spin decoupling effect. This would tend to make the decoupling requirement more severe, since in order to narrow the S spin resonance line appreciably, the rf field needs to be not only larger than the I - S interactions, but also larger than the "local field" of the I spins, i.e., $\omega_{1I} > \|\mathcal{H}_{IS}\|; \|\mathcal{H}_{II}\|$. For very large values of γ_I/γ_S where the flip-flop rate of the I spins becomes far more rapid than the heteronuclear coupling, a self-decoupling phenomenon can be observed. This leads to a narrowed S -spin resonance line, even when no rf field is applied to the I spins, as was observed for the ^{109}Ag NMR line in AgF.² The presence of strong dipolar interaction among the I spins therefore considerably modifies the dynamics of I - S interaction.⁵

This is observed even more dramatically, when a strong rf field is applied off resonance, i.e., under a certain angle ϑ_I in the I -spin rotating frame.¹⁶ Heteronuclear and homonuclear dipolar interaction are scaled differently in this case, thus the full dynamic range of the I -spin flip-flop motion can be controlled experimentally. This leads to interesting line-broadening and line-narrowing phenomena in the case of ^{109}Ag - ^{19}F and in the case of ^{13}C - ^1H in adamantane, as was shown recently.^{13,14} These effects are most pronounced when ϑ_I approaches the "magic angle" 54.7° where the I -spin flip-flop motion is quenched. The observation of heteronuclear dipolar inter-

action alone is feasible in this case.^{9,10}

In Sec. II, after introducing the interaction Hamiltonian in the tilted rotating frame, we first discuss the simple case of heteronuclear I - S interaction alone, i.e., $||\mathcal{H}_I||$ is assumed to be small compared with $||\mathcal{H}_{IS}||$. The free-induction decay (FID) and the corresponding spectrum can be calculated rigorously in this case, since only "two-body" interactions are involved.

However, if $||\mathcal{H}_I||$ becomes large compared with $||\mathcal{H}_{IS}||$ "many body" interactions among the I spins considerably modify the spin dynamics and no rigorous solution for the line shape can be obtained. In Sec. III we are therefore developing a line-shape theory, which allows to account for these many-body interactions by application of the "memory-function approach." A certain functional form for the memory function is assumed as the basic step in the approximation. Experimental details and the discussion of the experimental data are presented in Secs. IV and V.

II. SIMPLE THEORETICAL CONSIDERATIONS

Let us consider an abundant I -spin system with magnetogyric ratio γ_I dipolar coupled to S spins which are dilute and/or have a small gyromagnetic ratio γ_S , so that dipolar interaction among the S spins may be neglected compared with the I - S and the I - I interactions. A $\frac{1}{2}\pi$ pulse is applied in the y direction of the S spin rotating frame in order to induce a FID, whereas the I spins are continuously irradiated with an rf field $H_{1I} = \omega_{1I}/\gamma_I$ with frequency ω_I close to their Larmor frequency ω_{0I} . The following transformation (TR) leads now to the tilted doubly rotating frame:

$$T = e^{i\vartheta I^y}, \quad (1)$$

$$R = R_I R_S; \quad R_I = e^{-i\omega_I t I_x}; \quad R_S = e^{-i\omega_S t S_x}. \quad (2)$$

Defining

$$\Delta\omega_I = \omega_{0I} - \omega_I; \quad \omega_{eI}^2 = \Delta\omega_I^2 + \omega_{1I}^2; \quad \tan\vartheta_I = \omega_{1I}/\Delta\omega_I, \quad (3)$$

the total Hamiltonian in the TR frame is given by

$$\mathcal{H} = \mathcal{H}_I + \mathcal{H}_S + \mathcal{H}_{IS}, \quad (4)$$

with

$$\mathcal{H}_I = -\omega_{eI} I_x + P_2(\cos\vartheta_I) \mathcal{H}_I^{(2)} + \mathcal{H}_I^{(4)}, \quad (5a)$$

$$\mathcal{H}_S = -\omega_{0S} S_x, \quad (5b)$$

$$\mathcal{H}_{IS} = \cos\vartheta_I \mathcal{H}_{IS}^{(1)} - \sin\vartheta_I \mathcal{H}_{IS}^{(2)}, \quad (5c)$$

where

$$\mathcal{H}_I^{(2)} = \sum_{i < j} A_{ij} (3I_{zi} I_{zj} - \vec{I}_i \cdot \vec{I}_j), \quad (6a)$$

$$A_{ij} = -\gamma_I^2 \hbar \gamma_S^{-3} P_2(\cos\vartheta_{ij}). \quad (6b)$$

$\mathcal{H}_I^{(4)}$ contains the nonsecular terms, i.e.,

$$[I_x, \mathcal{H}_I^{(4)}] \neq 0; \quad [I_x, \mathcal{H}_I^{(2)}] = 0$$

and

$$\mathcal{H}_{IS}^{(1)} = \sum_{i,j} B_{ij} I_{zi} S_{zj}, \quad (7a)$$

$$\mathcal{H}_{IS}^{(2)} = \sum_{i,j} B_{ij} I_{xi} S_{zj}, \quad (7b)$$

$$B_{ij} = -2\gamma_I \gamma_S \hbar \gamma_{ij}^{-3} P_2(\cos\vartheta_{ij}). \quad (7c)$$

Here r_{ij} is the distance between spins i and j and ϑ_{ij} is the angle between the vector r_{ij} and the magnetic field H_0 where $P_2(\cos\vartheta)$ is the second Legendre polynomial. Note, that \mathcal{H}_{IS} does not commute with \mathcal{H}_I and \mathcal{H}_S respectively. The I and S spin reservoirs are therefore coupled by \mathcal{H}_{IS} .

The normalized free-induction decay of the S spins after the application of a $\frac{1}{2}\pi$ pulse in the y direction of their rotating frame is given by¹²

$$\langle S_x(t) \rangle = \langle S_x | \rho(t) \rangle / \langle S_x | \rho(0) \rangle, \quad (8)$$

where $\rho(t)$ is the time-dependent spin-density matrix in the TR frame and $\rho(0)$ its value immediately after the application of the rf pulse. We use here the notation¹²

$$\langle A | B \rangle \equiv \text{Tr}(A^\dagger B), \quad (9)$$

where A^\dagger is the adjoint of A . We shall also use the Liouville-operator definition^{17,18}

$$\hat{\mathcal{K}}|A\rangle = |[\mathcal{H}, A]\rangle \quad (10)$$

for any vector $|A\rangle$ in Liouville space. Within the "high-temperature approximation," which is valid for nuclear spins above 1 K at standard laboratory fields (≈ 6 T), Eq. (8) reduces to¹²

$$G(t) = \langle S_x | S(t) | S_x \rangle / \langle S_x | S_x \rangle, \quad (11)$$

where

$$S(t) = \exp(-it\hat{\mathcal{K}}), \quad (12)$$

and \mathcal{H} is given by Eq. (4).

The corresponding line shape $J(\omega)$ is obtained by Fourier transformation of Eq. (11):

$$J(\omega) = \int_0^\infty dt G(t) \cos\omega t. \quad (13)$$

However, Eqs. (11) and (12) cannot be solved exactly, because of the many-body character of the dipolar interaction $\mathcal{H}_I^{(2)}$ among the I spins. We will therefore have to resort to approximation schemes.

In order to demonstrate the essential difference between the two cases of strong or negligible dipolar coupling among the I spins, we shall treat the easiest case first, i.e., we neglect I - I spin couplings. This case is met in practice to a

certain degree, when I - S coupling is much stronger than the I - I coupling. If no radio-frequency field is applied to the I spins, the interaction among the I - S spins as represented by \mathcal{H}'_{IS} governs the S spin FID, which can be calculated rigorously by using

$$S(t) = \exp(-it\hat{\mathcal{H}}'_{IS}),$$

and Eq. (11) as¹

$$G_{IS}(t) = \prod_j \frac{\text{Tr}[\cos(B_j t I_{zj})]}{(2I+1)}, \quad (14)$$

where $G_{IS}(t)$ refers only to I - S coupling.

We obtain in this case for different values of I

$$I = \frac{1}{2}: G_{IS}(t) = \prod_j \cos(\frac{1}{2}B_j t), \quad (15)$$

$$I = 1: G_{IS}(t) = \prod_j \frac{1}{3}[1 + 2\cos(B_j t)], \quad (16)$$

$$I = \frac{3}{2}: G_{IS}(t) = \prod_j \frac{1}{2}[\cos(\frac{1}{2}B_j t) + \cos(\frac{3}{2}B_j t)]. \quad (17)$$

It is straightforward to calculate the FID of the S spin resonance for other I -spin quantum numbers according to Eq. (14).

Under the influence of the radio-frequency field, the I - S interaction becomes modulated in a coherent fashion, leading to "coherent averaging" of the Hamiltonian \mathcal{H}_{IS} .²¹ The FID of the S spins according to Eq. (11) is then governed by the time evolution operator

$$S(t) = T \exp\left(-i \int_0^t dt' \hat{\mathcal{H}}_{IS}(t')\right), \quad (18)$$

where T is a time-ordering operator and

$$\begin{aligned} \mathcal{H}_{IS}(t) = & \cos\vartheta_I \mathcal{H}'_{IS} \\ & - \sin\vartheta_I (\mathcal{H}^{(x\pi)}_{IS} \cos\omega_{eI}t + \mathcal{H}^{(y\pi)}_{IS} \sin\omega_{eI}t). \end{aligned} \quad (19)$$

Applying coherent averaging theory²¹ to Eq. (18) leads to a time evolution operator $S(t_c)$ given at integral increments of the cycle time $t_c = 2\pi/\omega_{eI}$ by

$$S(Nt_c) = \exp(-iNt_c \langle \hat{\mathcal{H}}_{IS} \rangle), \quad (20)$$

where

$$\langle \mathcal{H}_{IS} \rangle = \overline{\mathcal{H}}_{IS}^{(0)} + \overline{\mathcal{H}}_{IS}^{(1)} + \overline{\mathcal{H}}_{IS}^{(2)} + \dots \quad (21)$$

is given by a Magnus expansion.²¹

A lengthy but straightforward calculation leads to

$$\overline{\mathcal{H}}_{IS}^{(0)} = \cos\vartheta_I \sum_{i,j} B_{ij} I_{zi} S_{zj}, \quad (22)$$

$$\overline{\mathcal{H}}_{IS}^{(1)} = \sin\vartheta_I \frac{1}{\omega_{eI}} \sum_{i,j} B_{ij}^2 S_{zj}^2 (\cos\vartheta_I I_{xi} - \frac{1}{2} \sin\vartheta_I I_{zi}), \quad (23)$$

$$\begin{aligned} \overline{\mathcal{H}}_{IS}^{(2)} = & \sin\vartheta_I \frac{1}{\omega_{eI}^2} \sum_{i,j} B_{ij}^3 S_{zj}^3 [P_2(\cos\vartheta_I) I_{xi} \\ & - \cos\vartheta_I \sin\vartheta_I I_{zi}]. \end{aligned} \quad (24)$$

Higher-order terms may be calculated in a similar fashion. It is easily seen, that $\overline{\mathcal{H}}_{IS}^{(1)}$ does not contribute to a decay of the S -spin magnetization in the case of spin $S = \frac{1}{2}$, since $[S_x^2, S_x] = 0$. For the analogous reason, all odd-order terms in the Magnus expansion Eq. (12) do not contribute to the decay for $S = \frac{1}{2}$. If we restrict ourselves to spins $S = \frac{1}{2}$ we may ignore $\overline{\mathcal{H}}_{IS}^{(2k+1)}$ for integer k altogether, although cross terms with higher-order contributions have to be considered in principle. We now use the expression for $\overline{\mathcal{H}}_{IS}$ to discuss two limiting cases of interest in spin decoupling.

A. Off-resonance, with $\omega_{eI} \gg \|\mathcal{H}_{IS}\|$

Ignoring all higher-order terms is legitimate in this case and leaves as the leading term in $\overline{\mathcal{H}}_{IS}$:

$$\overline{\mathcal{H}}_{IS}^{(0)} = \cos\vartheta_I \mathcal{H}'_{IS}.$$

This is identical to the case of no rf irradiation except for the $\cos\vartheta_I$ term. Thus the same FID and corresponding S -spin line shape as in the case of no rf irradiation are expected but with the time and frequency axes scaled by $\cos\vartheta_I$ or its inverse, respectively. Thus the linewidth δ of the S -spin line can be expressed by

$$\delta/\delta_0 = \cos\vartheta_I = \Delta\omega / (\Delta\omega^2 + \omega_{eI}^2)^{1/2}, \quad (25)$$

where δ_0 is the full uncoupled S linewidth. No special line-shape theory has to be applied, since the corresponding line shape can be calculated rigorously by using Eq. (14) and replacing B_j by $\cos\vartheta_I B_j$. In the case that ω_{eI} is not large compared with $\|\mathcal{H}_{IS}\|$ higher-order correction terms in the Magnus expansion may be taken into account

B. On-resonance, i.e., $\Delta\omega = 0, \vartheta_I = 90^\circ$

Note that $\overline{\mathcal{H}}_{IS}^{(0)}$ vanishes in this case and the effective Hamiltonian may be written, according to Eqs. (23) and (24) as the sum of the two leading terms

$$\overline{\mathcal{H}}_{IS}^{(1)} = -\frac{1}{2\omega_{eI}} \sum_{i,j} B_{ij}^2 I_{zi} S_{zj}^2, \quad (26)$$

$$\overline{\mathcal{H}}_{IS}^{(2)} = -\frac{1}{2\omega_{eI}^2} \sum_{i,j} B_{ij}^3 I_{xi} S_{zj}^3. \quad (27)$$

Since $\overline{\mathcal{H}}_{IS}^{(1)}$ and other odd-order terms in the Magnus expansion do not contribute to the decay of S spin magnetization in the case of $S = \frac{1}{2}$, we may calculate the FID by using just the leading term $\overline{\mathcal{H}}_{IS}^{(2)}$. The Magnus expansion however does

not converge rapidly for $\omega_{1I} < |\mathfrak{H}_{IS}^c|$. We therefore have to distinguish two limiting cases, namely, (a) $\omega_{1I} \geq |\mathfrak{H}_{IS}^c|$ and (b) $\omega_{1I} \leq |\mathfrak{H}_{IS}^c|$. In case (a) we may proceed according to Eqs. (11) and (12) with $\mathfrak{H}_{IS}^{(2)}$ as the leading interaction Hamiltonian. Under this assumption $G_{IS}(t)$ can be readily calculated as described above, which in the case of $S = \frac{1}{2}$ results in

$$G_{IS}(t) = \prod_j \frac{\text{Tr}[\cos(B_j^* I_{zj})]}{(2I+1)}, \quad (28)$$

with

$$B_j^* = B_j \frac{1}{2} (B_j / 2\omega_{1I})^2, \quad (29)$$

i.e., each lattice parameter B_j is scaled by the factor $\lambda_j = \frac{1}{2} (B_j / 2\omega_{1I})^2$. Note that within this approximation (truncation of the Magnus expansion at $\mathfrak{H}^{(2)}$) the FID of the S -spin resonance and correspondingly the line shape can be calculated rigorously for a given spin system, by using just the lattice parameters B_j . Equation (28), on the other hand, represents the FID in the case of no rf irradiation when B_j^* is replaced by B_j . We therefore propose, to use Eq. (28) over the full range of ω_{1I} values, by expressing B_j^* as

$$B_j^* = \epsilon_j B_j, \quad (30)$$

where

$$\epsilon_j = \lambda_j / (1 + \lambda_j), \quad (31)$$

which gives the correct FID in the two limiting cases of $\lambda_j \gg 1$ and $\lambda_j \ll 1$ and may be a reasonably good approximation for $\lambda_j \approx 1$. The line shape and its width may be calculated from Eqs. (28) and (30) numerically. However it may be more convenient in practical applications, to have a simple formula for the linewidth. We therefore assume a Gaussian FID with the second moment

$$M_2 = \frac{1}{3} I(I+1) \sum_j \epsilon_j^2 B_j^2, \quad (32)$$

resulting in the linewidth at half height of $\delta = 1.18 M_2^{1/2}$ or with $\Delta\nu = \delta/\pi$ for the full linewidth at half-height in hertz as

$$\Delta\nu = 0.3756 M_2^{1/2}. \quad (33)$$

III. LINE-SHAPE THEORY

Whereas the line shape of the S -spin NMR signal could be calculated rigorously under the condition of negligible I - I coupling as shown in Sec. II, we shall have to apply approximation schemes, when we calculate the line shape under the condition of strong I - I coupling. Dramatic effects will be seen on the S -spin resonance signal due to I - I coupling. We shall derive now an exact integrodifferential equation for the free-induction

decay, which contains a kernel $K(t)$, sometimes called the "memory function" since it represents memory effects in the interaction.^{18,19} This memory function is discussed for different experimental situations and approximated only in the final step, by choosing a certain functional form, fitted to the correct second moment. We note that for certain experimental conditions, the memory function can be calculated rigorously as will be seen later. Using the projector¹²

$$P = \frac{|S_x\rangle\langle S_x|}{\langle S_x | S_x \rangle}, \quad (34)$$

we are able to obtain an integrodifferential equation for the FID of the S spins as follows^{12,18,19}.

$$\frac{d}{dt} G(t) = - \int_0^t dt' K(t') G(t-t'), \quad (35)$$

with the memory function

$$K(t) = \frac{\langle S_x | \mathfrak{H}_{IS}^c S(t) \mathfrak{H}_{IS}^c | S_x \rangle}{\langle S_x | S_x \rangle}, \quad (36)$$

with

$$S(t) = \exp\{-it[\hat{\mathfrak{H}}_I + (1-P)\hat{\mathfrak{H}}_{IS}]\}, \quad (37)$$

where \mathfrak{H}_I and \mathfrak{H}_{IS} are given by Eqs. (5) and (7). The free-induction decay is therefore fully determined by the knowledge of $K(t)$. If the memory function $K(t)$ is known, whether exactly or in some degree of approximation, the NMR line shape $J(\omega)$ may be calculated by Laplace inversion, as follows¹⁸:

$$J(z) = [z + K(z)]^{-1}, \quad (38a)$$

with

$$J(z) = \mathcal{L}[G(t)] \quad (38b)$$

and

$$K(z) = \mathcal{L}[K(t)], \quad (38c)$$

from which the NMR line shape according to Eq. (13) may be calculated as¹⁸

$$J(\omega) = \frac{K'(\omega)}{[\omega - K''(\omega)]^2 + K'^2(\omega)}, \quad (39a)$$

with

$$K'(\omega) = \int_0^\infty dt K(t) \cos \omega t, \quad (39b)$$

$$K''(\omega) = \int_0^\infty dt K(t) \sin \omega t. \quad (39c)$$

Note that an exponential FID and a Lorentzian line shape results, if $K(t)$ is a δ function. For illustrative purposes, we have plotted in Fig. 1 a Gaussian and a Lorentzian FID $G(t)$ together with their memory functions $K(t)$. The memory func-

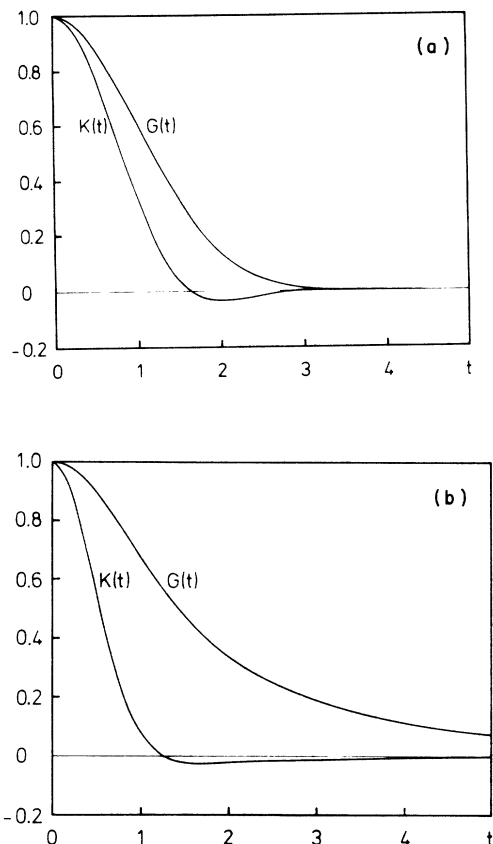


FIG. 1. Free-induction decay $G(t)$ and corresponding memory function $K(t)$ as calculated according to Eq. (40). (a) Gaussian FID $G(t) = e^{-t^2/2}$; (b) Lorentzian FID $G(t) = [1 + \frac{1}{2}t^2]^{-1}$.

tion $K(t)$ in each case was determined numerically by using the following iteration procedure¹²:

$$K(t) = - \int_0^t dt' K(t')G'(t-t') - G''(t), \quad (40)$$

where $G'(t)$ and $G''(t)$ are the first and second time derivative of the free-induction decay $G(t)$. Figure 1 shows that $K(t)$ has a zero crossing in both cases, whereas $G(t)$ is a monotonic function. In general, $K(t)$ will have more nodes than the original function $G(t)$. A further general aspect is clearly demonstrated in Fig. 1, i.e., the rapid decay of $K(t)$ on a shorter time scale than $G(t)$. Let us now discuss some special experimental situations.

A. No rf field applied to the I spins ($\omega_{1I} = 0, \vartheta_I = 0$)

This corresponds to the ordinary NMR line shape of S spins, governed by the I - S dipolar interaction with abundant I spins. This case has been investigated experimentally by Abragam and

Winter² in the case of ^{109}Ag in AgF . Walstedt²⁰ has given a theoretical account of the dynamics involved in a slightly different manner than is described here.

As shown above, we only have to find the corresponding memory function $K(t)$, from which the line shape $J(\omega)$ according to Eq. (39) may be calculated. With $\omega_{1I} = 0, \vartheta_I = 0$ we obtain from Eq. (5),

$$\mathcal{H}_I = \mathcal{H}'_{II}, \quad \mathcal{H}_{IS} = \mathcal{H}'_{IS}.$$

This may be inserted into Eqs. (36) and (37) in order to obtain the corresponding expression for the memory function. Before we discuss the functional form of $K(t)$ in more detail, we proceed to the next more-general case (B), from which case (A) may be obtained in the limit of $\vartheta_I = 0$.

B. Strong rf irradiation: $\omega_{1I} \gg \|\mathcal{H}'_{II}\| : \|\mathcal{H}'_{IS}\|$

The time evolution operator $S(t)$ according to Eq. (37) is now expressed by

$$S(t) = \exp\left\{-it\left[-\omega_{eI}\hat{I}_z + P_2(\cos\vartheta_I)\hat{\mathcal{H}}'_{II} + \hat{\mathcal{H}}^*_{II} + (1-P)\cos\vartheta_I\hat{\mathcal{H}}'_{IS}\right]\right\}, \quad (41)$$

where the corresponding Hamiltonians are defined by Eqs. (5)–(7). This propagator may be formally split into a product form as follows²¹:

$$S(t) = S_2(t)S_1(t), \quad (42a)$$

with

$$S_2(t) = \exp(it\omega_{eI}\hat{I}_z) \quad (42b)$$

and

$$S_1(t) = T \exp\left(-i \int_0^t dt' \hat{\mathcal{H}}(t')\right), \quad (42c)$$

where

$$\hat{\mathcal{H}}(t) = S_2^{-1}(t)\left[P_2(\cos\vartheta_I)\hat{\mathcal{H}}'_{II} + \hat{\mathcal{H}}^*_{II} + (1-P)\cos\vartheta_I\hat{\mathcal{H}}'_{IS}\right]S_2(t). \quad (42d)$$

The interaction Hamiltonian $\hat{\mathcal{H}}(t)$ which is modulated by ω_{eI} may be separated into a time-independent (secular) and a time-dependent (nonsecular) part

$$\hat{\mathcal{H}}(t) = P_2(\cos\vartheta_I)\hat{\mathcal{H}}'_{II} + (1-P)\cos\vartheta_I\hat{\mathcal{H}}'_{IS} + \hat{\mathcal{H}}^*_{II}(t) + \hat{\mathcal{H}}^*_{IS}(t), \quad (43)$$

where the nonsecular parts oscillate with frequency ω_{eI} and $2\omega_{eI}$, respectively. Because of the condition $\omega_{eI} \gg \|\hat{\mathcal{H}}'_{II}\|, \|\hat{\mathcal{H}}'_{IS}\|$ the first-order contribution to the average Hamiltonian in a Magnus expansion of $S_1(t)$ becomes rather small and we may approximate $\hat{\mathcal{H}}(t)$ by the time averaged Hamiltonian,²¹ which results in

$$S_1(t) \approx S_0(t) = \exp\{-it[P_2(\cos\vartheta_I)\hat{\mathcal{C}}'_{II} + (1-P)\cos\vartheta_I\hat{\mathcal{C}}'_{IS}]\}. \quad (44)$$

After some algebraic manipulation, the memory function $K(t)$ according to Eq. (36) may now be expressed by¹²

$$K(t) = \cos^2\vartheta_I K_x(t) + \sin^2\vartheta_I K_y(t) \cos\omega_{eI}t, \quad (45)$$

with

$$K_x(t) = \frac{(S_x|\hat{\mathcal{C}}'_{IS}S_0(t)\hat{\mathcal{C}}'_{IS}|S_x)}{(S_x|S_x)} \quad (46)$$

and

$$K_y(t) = \frac{(S_x|\hat{\mathcal{C}}'_{IS}^{(xz)}S_0(t)\hat{\mathcal{C}}'_{IS}^{(xz)}|S_x)}{(S_x|S_x)}. \quad (47)$$

Under the condition $\omega_{eI} \gg \|\hat{\mathcal{C}}'_{II}\|; \|\hat{\mathcal{C}}'_{IS}\|$ discussed here, the second term of $K(t)$ in Eq. (45) does not contribute appreciably to $K'(\omega)$ and $K''(\omega)$ and will be neglected here. It is, however, straightforwardly included if this is felt to be appropriate, e.g., when ω_{eI} is not large enough and neglecting this term is not justified.

We summarize now, by stating that under the condition of strong rf irradiation close to the I -spin Larmor frequency, the memory function may be represented by

$$K_0(t) = \cos^2\vartheta_I \frac{(S_x|\hat{\mathcal{C}}'_{IS}S_0(t)\hat{\mathcal{C}}'_{IS}|S_x)}{(S_x|S_x)}, \quad (48)$$

with $S_0(t)$ given by Eq. (44).

Note that $K_0(t)$ is the corresponding memory function of the S -spin line shape when no rf irradiation is applied to the I spins as discussed in case (A), with $\vartheta_I = 0$. On the other hand, $K_0(t)$ vanishes identically, if $\vartheta_I = 90^\circ$. The correspond-

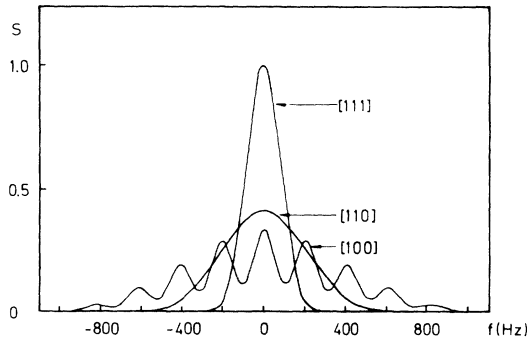


FIG. 2. Calculated line shape $J(\omega)$ of an "isolated" S spin surrounded by abundant I spins in NaCl-type cubic lattice for three different orientations of the magnetic field H_0 under the condition of quenched I - I interactions. The frequency axis is chosen for the case of ^{109}Ag resonance in AgF.

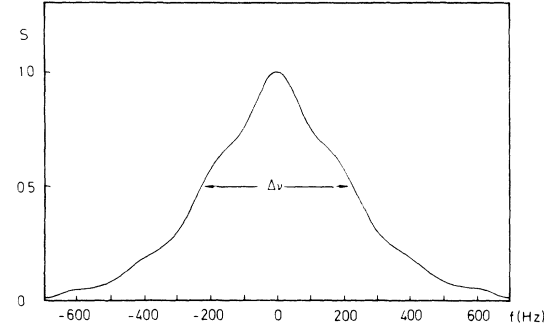


FIG. 3. Powder line shape $J(\omega)$ under the condition of quenched I - I interaction ($\vartheta_I = 54.7^\circ$) in the case of ^{109}Ag resonance in AgF.

ing line shape is a δ function with zero halfwidth, i.e., the I spins are completely decoupled. A further interesting limiting case is reached, when ϑ_I equals the magic angle, where $P_2(\cos\vartheta_I) = 0$, i.e., $\cos^2\vartheta_I = \frac{1}{3}$. In this case the FID can be calculated rigorously as was shown in Sec. II:

$$G_{IS}(t) = (S_x|\exp(-it/\sqrt{3})\hat{\mathcal{C}}'_{IS}|S_x)/(S_x|S_x), \quad (49)$$

with $G_{IS}(0) = 1$, and which results in

$$G_{IS}(t) = \prod_j \frac{\text{Tr}[\cos(B_j 3^{-1/2} t I_{ej})]}{(2I+1)}. \quad (50)$$

In the case $I = \frac{1}{2}$ we obtain

$$G_{IS}(t) = \prod_j \cos(\frac{1}{2} 3^{-1/2} B_j t). \quad (51)$$

The corresponding rigorous memory function $K_{IS}(t)$ can be calculated numerically by using Eq. (40).

The pure I - S dipolar spectrum (i.e., with no I - I couplings) in a NaCl-type lattice has been calculated for three different orientations of the magnetic field H_0 as displayed in Fig. 2. For the $[100]$ orientation of the magnetic field, a discrete pattern emerges due to the six nearest neighbors. This structure is still partially retained in a powder average (Fig. 3), where different spectra for a random distribution of magnetic field orientations are averaged. No simple functional form can be assumed for the memory function $K_{IS}(t)$ of the I - S dipolar FID $G_{IS}(t)$ as is demonstrated in Fig. 4 in the case of H_0 parallel to the $[100]$ direction. $K_{IS}(t)$ in Fig. 4 has been calculated numerically by the procedure outlined above [see Eq. (40)]. It should be noted, that the corresponding spectrum $J(\omega)$ as shown in Fig. 2 can be obtained by Fourier transformation of $G_{IS}(t)$ or by using $K_{IS}(t)$ and applying Eqs. (38) and (39).

However, the full memory function $K_0(t)$ accord-

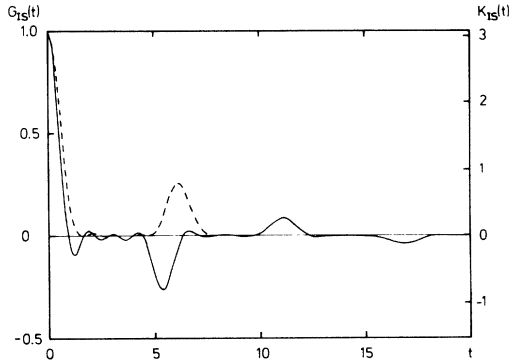


FIG. 4. Free-induction decay $G_{IS}(t)$ of the S-spin resonance (dashed curve) under pure I -S interaction as calculated according to Eq. (15) for an NaCl-type lattice, with the magnetic field in the [100] direction. The Fourier transform of $G_{IS}(t)$ is represented in Fig. 2. The corresponding memory function $K_{IS}(t)$ (solid line) was calculated according to Eq. (40). The time axis is drawn in units of $[(1/\sqrt{3})(\gamma_I \gamma_S \hbar/a^3)]^{-1}$.

ing to Eq. (48) cannot be calculated exactly, and we are setting out to employ some approximations in the following. We note, that an expansion of $K_0(t)$ in powers of t can be performed rigorously, which leads to¹²

$$K_0(t) = K(0) \sum_{n=0}^{\infty} \frac{(-it)^n}{n!} N_n, \quad (52)$$

with

$$\begin{aligned} K(0) &= \cos^2 \vartheta_I \frac{\langle S_x | \hat{\mathcal{J}}_{IS}'^2 | S_x \rangle}{\langle S_x | S_x \rangle} \\ &= \cos^2 \vartheta_I M_2^{IS}, \end{aligned} \quad (53)$$

and where

$$N_n = \frac{\langle S_x | \hat{\mathcal{J}}_{IS}' [P_2(\cos \vartheta_I) \hat{\mathcal{J}}_{IS}' + (1-P) \cos \vartheta_I \hat{\mathcal{J}}_{IS}']^n \hat{\mathcal{J}}_{IS}' | S_x \rangle}{(\hat{\mathcal{J}}_{IS}' | \hat{\mathcal{J}}_{IS}')}. \quad (54)$$

It can be shown, that the moments N_n vanish for odd n . For the second moment we obtain

$$N_2 = M_2^{IS} [P_2^2(\cos \vartheta_I) \mu_2 + \cos^2 \vartheta_I (\mu_1 - 1)], \quad (55)$$

where

$$\mu_2 = \frac{M_4^{IIS}}{(M_2^{IS})^2} \quad \text{and} \quad \mu_1 = \frac{M_4^{SIS}}{(M_2^{IS})^2}, \quad (56)$$

with

$$\begin{aligned} M_4^{IIS} &= \frac{\langle S_x | \hat{\mathcal{J}}_{IS}' \hat{\mathcal{J}}_{IS}'^2 \hat{\mathcal{J}}_{IS}' | S_x \rangle}{\langle S_x | S_x \rangle}, \\ M_4^{SIS} &= \frac{\langle S_x | \hat{\mathcal{J}}_{IS}'^4 | S_x \rangle}{\langle S_x | S_x \rangle}. \end{aligned} \quad (57)$$

The second and fourth moments M_2 and M_4 are readily calculated for a specific spin system by

evaluation of the corresponding lattice sums S_i ,¹²

$$M_2^{IS} = \frac{4}{3} I(I+1) d^2 S_1, \quad (58)$$

$$\begin{aligned} M_4^{SIS} &= \frac{16}{3} I(I+1) d^4 \\ &\times \left[\frac{1}{5} (3I^2 + 3I - 1) S_2 + I(I+1)(S_1^2 - S_2) \right], \end{aligned} \quad (59)$$

$$M_4^{IIS} = 2 \left[\frac{2}{3} I(I+1) \right]^2 d^4 (\gamma_I / \gamma_S)^2 (S_4 - S_3), \quad (60)$$

with

$$d = \gamma_I \gamma_S \hbar / a^3, \quad (61)$$

where a is the lattice constant and

$$S_1 = \sum_i b_i^2, \quad S_2 = \sum_i b_i^4, \quad (62)$$

$$S_3 = \sum_{i \neq j} b_{ij}^2 b_i b_j, \quad S_4 = \sum_{i \neq j} b_{ij}^2 b_i^2,$$

with

$$b_i = P_2(\cos \vartheta_i) r_i^{-3},$$

$$b_{ij} = P_2(\cos \vartheta_{ij}) r_{ij}^{-3},$$

where r_i is the distance between I and S spins and r_{ij} the distance between I_i and I_j spins, defined in units of the lattice constant a .

Higher-order even moments may be obtained by a tedious, but straightforward calculation.⁸ However, this usually employs considerable computational effort and we prefer to approximate the memory function $K_0(t)$ by using just $K(0)$ and the second moment N_2 according to Eq. (55).¹⁴

Before approximating the memory function $K_0(t)$, let us take a look at the correlation time τ_c of the I - S coupling due to the spin flip-flop motion of the I spins. With¹³

$$1/\tau_c^2 = P_2(\cos \vartheta_I)^2 / \tau_{c0}^2, \quad (63a)$$

where

$$1/\tau_{c0}^2 = M_4^{IIS} / 2M_2^{IS}, \quad (63b)$$

the correlation time can be scaled at the experimenters will by varying the angle ϑ_I of the effective field in the rotating frame of the I spins. Especially at the magic angle $\vartheta_I = 54.7^\circ$ this correlation time becomes infinite and the flip-flop motion of the I spins is quenched. In Fig. 5(a) we have plotted τ_c vs ϑ_I in the case of AgF for three different orientations of the magnetic field according to Eq. (63). The divergence of τ_c at the magic angle is clearly evident. The orientational dependence of τ_c is not very pronounced.

Let us define the line-narrowing parameter

$$\Delta = M_2^{1/2} \tau_c, \quad (64a)$$

with

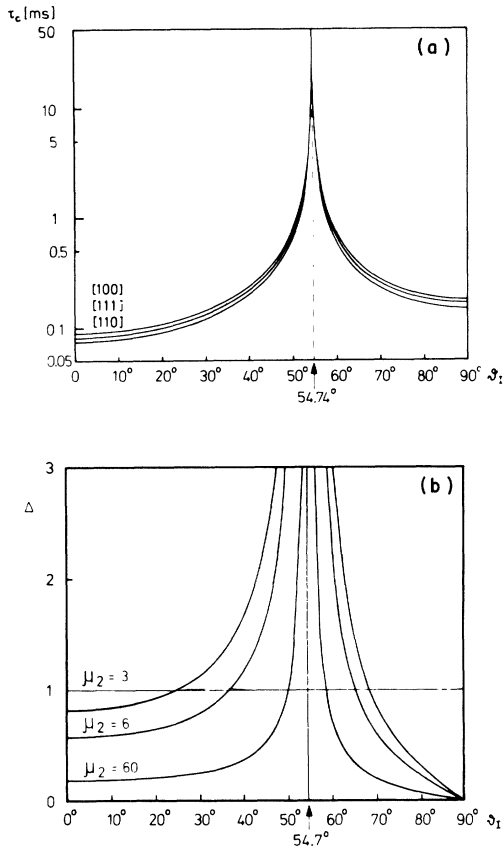


FIG. 5. (a) Correlation time τ_c of the flip-flop motion of the ^{19}F - ^{109}Ag interaction in AgF for three different magnetic field orientations versus the angle ϑ_I of the effective field in the rotating frame of the ^{19}F spins as calculated by using Eq. (63). (b) Linewidth parameter $\Delta = M_2^{1/2}\tau_c$ according to Eq. (64) vs ϑ_I for three different values of μ_2 , where $\mu_2 = 60$ corresponds to the AgF case, whereas $\mu_2 = 6$ represents the adamantane case. The straight line ($\Delta = 1$) separates the two regimes of motion ($\Delta \ll 1$ extreme narrowing; $\Delta \gg 1$ rigid case).

$$M_2 = \cos^2 \vartheta_I M_2^S. \quad (64b)$$

Using Eqs. (56) and (63) this may be expressed as

$$\Delta = \frac{\cos \vartheta_I}{|P_2(\cos \vartheta_I)|} \left(\frac{2}{\mu_2} \right)^{1/2}. \quad (64c)$$

This line-narrowing parameter Δ separates the different regimes of spin motion ($\Delta \ll 1$ extreme narrowing, $\Delta \gg 1$ rigid case) and is plotted versus ϑ_I in Fig. 5(b). After this qualitative discussion we set out to calculate the line shape of the S spins by having only knowledge of the initial value $K(0)$ [Eq. (53)] of the memory function $K_0(t)$ and its second moment N_2 [Eq. (55)]. If only this information is available, the best guess for the functional form of $K_0(t)$ is a Gaussian according to information theory,⁸ i.e.,

$$K_0(t) = K(0) \exp(-\frac{1}{2} N_2 t^2). \quad (65)$$

The line shape $J(\omega)$ of the S-spin NMR signal is readily calculated under this assumption by making use of Eqs. (39), (55), and (65), where the sine and cosine transform of $K_0(t)$,¹⁸

$$K'_0(\omega) = K(0) (\pi/2N_2)^{1/2} e^{-\omega^2/2N_2}, \quad (66a)$$

$$K''_0(\omega) = K(0) (\omega/N_2) e^{-\omega^2/2N_2} F(\frac{1}{2}; \frac{3}{2}; \omega^2/2N_2), \quad (66b)$$

have to be inserted and where $F(\frac{1}{2}; \frac{3}{2}; \omega^2/2N_2)$ is the confluent hypergeometric function, which is tabulated and can be calculated numerically.

Very often a simple expression for the linewidth is wanted, which can be compared with experimental data. Defining the halfwidth at half-height of $J(\omega)$ as δ , we arrive at the expression¹²

$$\delta = [\pi K(0)/2N_2]^{1/2} f(\mu), \quad (67)$$

where $f(\mu)$ is a function of the parameter $\mu = M_4/M_2^2$, which approaches $f(\mu) = 1$ for $\mu \gg 3$ and in the case of $J(\omega)$ being Gaussian ($\mu = 3$) reaches the value $f(3) = 1.5$.

We believe that Eq. (67) with $f(\mu) = 1$ gives a simple, but accurate enough expression for the linewidth of more or less Lorentzian line shapes. Using Eqs. (53), (55), and (67) we arrive at¹²

$$\delta = \left(\frac{\pi}{2} \right)^{1/2} \left(\frac{\cos^4 \vartheta_I M_2^S}{P_2^2(\cos \vartheta_I) \mu_2 + \cos^2 \vartheta_I (\mu_1 - 1)} \right)^{1/2}, \quad (68)$$

which represents the linewidth variation of the S-spin NMR signal $J(\omega)$ with varying angle ϑ_I of the effective field in the rotating frame of the I spins. The limiting case of (a) no rf irradiation of the I spins, i.e., $\vartheta_I = 0$, (b) irradiation at the magic angle $\cos^2 \vartheta_I = \frac{1}{3}$, and (c) on-resonance decoupling $\vartheta_I = \frac{1}{2}\pi$; $\delta = 0$ are included. We note, however, that Eq. (68) should be applied with care in the case of a powder sample, since the halfwidth of the averaged line shapes does not agree with the width corresponding to average moments, if the moments vary appreciably with the orientation of the magnetic field. Note that Eq. (68) is very similar to the linewidth expression obtained for a truncated Lorentzian line shape.¹

We note, that the linewidth δ according to Eq. (68) does not at all vary as $\cos \vartheta_I$, which was the case treated in Sec. II, where I-I couplings were neglected. The memory function $K_0(t)$, Eq. (48), on the other hand resembles very much the correlation function which governs the cross relaxation between I and S spins in the case of an ADRF-type double resonance experiments.^{5,8} In fact, $K_0(t)$ is identical with this correlation function if $\|\mathcal{H}'_{IS}\|$ is small compared with $\|\mathcal{H}'_{II}\|$. McArthur, Hahn, and Walstedt⁵ have shown that in CaF₂ the experimental data are fitted quite nicely to a Lorentzian

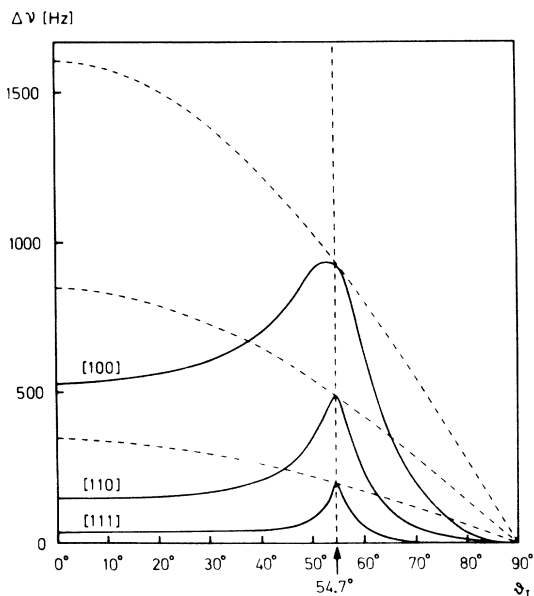


FIG. 6. Excess linewidth $\Delta\nu$ of ^{109}Ag resonance in AgF for three different orientations of the magnetic field versus the angle ϑ_I of the effective field in the rotating frame of the ^{19}F spins as calculated by the mixed memory-function approach, where $K_{II}(t)$ is Lorentzian (see text).

correlation function. This has also been confirmed in another system.^{7,22}

Moreover, Demco, Tegenfeldt, and Waugh⁸ have made a detailed analysis of this correlation function by applying the memory-function approach. The same approach can be applied to $K_0(t)$, but this amounts to quite a heavy computational effort.⁸ Excluding the region close to the magic angle it may be a reasonable approximation therefore to express $K_0(t)$ as a Lorentzian:

$$K_0(t) = K(0)(1 + \frac{1}{2}N_2 t^2)^{-1}. \quad (69)$$

An analytic expression for $J(\omega)$ is obtained according to Eq. (39) by using

$$K'_0(\omega) = K(0)\pi(2N_2)^{-1/2} e^{-x}, \quad (70)$$

$$K''_0(\omega) = K(0)(2N_2)^{-1/2} \times [\exp(-x)E^*(x) - \exp(x)Ei(-x)], \quad (71)$$

with $x = \omega(2/N_2)^{1/2}$, and where $Ei(-x)$ and $E^*(x)$ are the exponential integrals.²³ The linewidth δ may be determined directly from the lineshape $J(\omega)$. As we have remarked already this may be a poor approximation at the magic angle. This is especially annoying since we have demonstrated above that the memory function can be calculated exactly at the magic angle.

We are therefore led to express $K_0(t)$ by the product

$$K_0(t) = K_{II}(t)K_{IS}(t), \quad (72)$$

with

$$K_{II}(t) = \frac{(S_x | \hat{\mathcal{H}}'_{IS} \exp[-itP_2(\cos\vartheta_I)\hat{\mathcal{H}}'_{II}] \hat{\mathcal{H}}'_{IS} | S_x)}{(\hat{\mathcal{H}}'_{IS} | \hat{\mathcal{H}}'_{IS})} \quad (73)$$

and

$$K_{IS}(t) = \cos^2\vartheta_I \times \frac{(S_x | \hat{\mathcal{H}}'_{IS} \exp[-it\cos\vartheta_I(1-P)\hat{\mathcal{H}}'_{IS}] \hat{\mathcal{H}}'_{IS} | S_x)}{(S_x | S_x)}. \quad (74)$$

At the magic angle, $K_{II}(t) = 1$ and $K_0(t)$ is equal to the memory function $K_{IS}(t)$, which may be calculated numerically as outlined above [Eq. (40)] and as is demonstrated in Figs. 1 and 4. For all other values of ϑ_I this is a good approximation if higher-order correlations are neglected. Note that $K_{II}(t) = 1$, i.e., is independent of time if all B_i are equal. Thus only the difference in the B_i values for two I spins coupled to the S spin causes a destruction of $K_{II}(t)$. This fact seems to favor a Lorentzian shape for $K_{II}(t)$. For comparison also a Gaussian form for $K_{II}(t)$ has been used. In both cases only the second moment of $K_{II}(t)$ needs to be evaluated. This mixed memory-function approach [Eq. (72)] using a Lorentzian or a Gaussian functional form of $K_{II}(t)$ and calculating $K_{IS}(t)$ rigorously is applied to AgF and adamantane. Figure 6 displays the linewidth $\Delta\nu = \delta/\pi$ of the ^{109}Ag excess line shape in AgF over the full range of ϑ_I values for three different orientations of the magnetic field as calculated by making use of the mixed memory function approach. The dramatical orientation dependence of the linewidth should be noted and special attention is drawn to the significant line broadening, which is observed when ϑ_I approaches the magic angle. Let us now discuss the case of on-resonance decoupling.

C. On-resonance decoupling, $\vartheta_I = \frac{1}{2}\pi, \omega_{II}$ arbitrary

We start with Eqs. (36) and (37), where we use in the rotating frame

$$\hat{\mathcal{H}}_I = -\omega_{II}I_x + \hat{\mathcal{H}}'_{II}, \quad \hat{\mathcal{H}}_{IS} = \hat{\mathcal{H}}'_{IS}.$$

This results in

$$K(t) = \frac{(S_x | \hat{\mathcal{H}}'_{IS} S(t) \hat{\mathcal{H}}'_{IS} | S_x)}{(S_x | S_x)}, \quad (75)$$

with

$$S(t) = \exp\{-it[-\omega_{II}\hat{I}_x + \hat{\mathcal{H}}'_{II} + (1-P)\hat{\mathcal{H}}'_{IS}]\}. \quad (76)$$

Expressing $S(t)$ analogously to Eq. (42) as a product of two time-evolution operators $S_2(t)$. $S_1(t)$ leads to

$$K(t) = K_1(t) \cos \omega_{1I} t, \quad (77)$$

with

$$K_1(t) = \frac{(S_x | \hat{\mathcal{C}}'_{IS} S_1(t) \hat{\mathcal{C}}'_{IS} | S_x)}{(S_x | S_x)}, \quad (78)$$

where

$$S_1(t) = T \exp \left(-i \int_0^t dt' \hat{\mathcal{C}}(t') \right), \quad (79)$$

$$\hat{\mathcal{C}}(t) = e^{-i\omega_{1I} t} [\hat{\mathcal{C}}'_{II} + (1-P)\hat{\mathcal{C}}'_{IS}] e^{i\omega_{1I} t}.$$

Two limiting cases arise:

(a) $\omega_{1I} \ll \|\hat{\mathcal{C}}'_{IS}\|; \|\hat{\mathcal{C}}'_{II}\|$, i.e., $S_1(t)$ reduces to

$$S_1(t) = \exp \left\{ -it [\hat{\mathcal{C}}'_{II} + (1-P)\hat{\mathcal{C}}'_{IS}] \right\}. \quad (80)$$

$K_1(t)$ therefore equals $K_0(t)$ according to Eq. (47) with $\vartheta_I = 0$. As suggested earlier a valid approximation procedure would be to assume a Lorentzian shape for $K_0(t)$ or to use the mixed memory-function approach.

(b) $\omega_{1I} \gg \|\hat{\mathcal{C}}'_{IS}\|; \|\hat{\mathcal{C}}'_{II}\|$, i.e., $S_1(t)$ reduces to

$$S_1(t) = \exp(it \frac{1}{2} \hat{\mathcal{C}}'_{II}), \quad (81)$$

with

$$\hat{\mathcal{C}}'_{II} = \sum_{i < j} A_{ij} (3I_{xi} I_{xj} - \vec{I}_i \cdot \vec{I}_j)$$

and where nonsecular terms have been neglected. The corresponding memory function is now different in structure compared with $K_0(t)$ or with $K_x(t)$ for $\vartheta_I = \frac{1}{2} \pi$ [Eq. (46)]. However there is a basic difference in structure, since $K_{II}(t)$ is constant if all B_i are equal, whereas $K_1(t)$ with $S_1(t)$ as given by Eq. (81) under the same condition would just be $K(0)$ times the free-induction decay of the I spins with a time axis scaled by a factor of 2. In closed-packed cubic solids the FID is close to a Gaussian. As a first-order approximation we would therefore assume $K_x(t)$ to be Gaussian with the second moment

$$N_{2x} = \frac{1}{4} M_{4x}^{IIIS} / M_2^{IS}, \quad (82)$$

where

$$M_{4x}^{IIIS} = \frac{(S_x | \hat{\mathcal{C}}'_{IS} \hat{\mathcal{C}}'_{II} \hat{\mathcal{C}}'_{IS} | S_x)}{(S_x | S_x)}, \quad (83)$$

which is readily calculated to be¹²

$$M_{4x}^{IIIS} = \left[\frac{2}{3} I(I+1) \right]^2 d^4 (\gamma_I / \gamma_S)^2 (5S_4 + 4S_3), \quad (84)$$

where the lattice sums S_4 and S_3 are defined by Eq. (62).

(c) $\omega_{1I} \approx \|\hat{\mathcal{C}}'_{IS}\|; \|\hat{\mathcal{C}}'_{II}\|$: In this case, we may approximate $S_1(t)$ by

$$S_1(t) \approx \exp(-it \hat{\mathcal{C}}'_{II}), \quad (85)$$

with $K_1(t)$ assumed to be Gaussian or Lorentzian. All three cases do give very similar results and

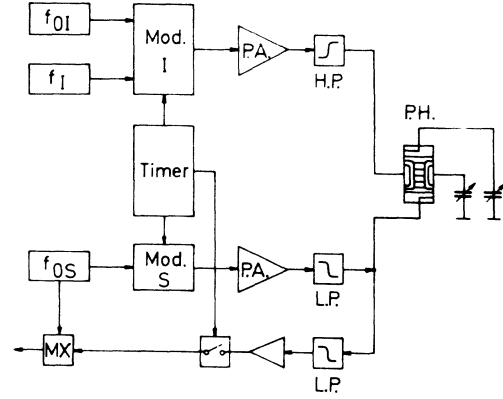
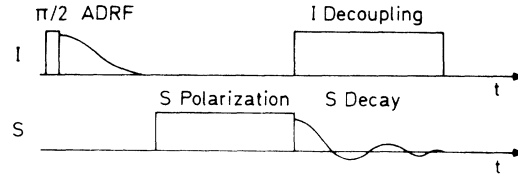


FIG. 7. Experimental setup and schematic representation of the pulse timing as used in a one-shot cross polarization experiment, followed by continuous decoupling (Refs. 6 and 12). Mod., Phase modulator; P.A., power amplifier; H.P., high pass filter; L.P., low pass filter; P.H., probe head; MX, mixer; f_{0I} , f_{0I} , and f_{0S} : frequency generators).

cover the whole range of ω_{1I} values. Case (c), however, seems to be the most reasonable approximation, when compared with experimental data. Application of this theory to spin-decoupling experiments is discussed in Sec. V.

IV. EXPERIMENTAL

Experiments were performed on AgF and adamantane ($C_{10}H_{16}$) powder. The samples were used as obtained from Merck GmbH, Darmstadt. A Bruker magnet system (2.114 T) and a Bruker pulse spectrometer (SXP 4-100) in combination with a home-built double-resonance setup were used to generate the necessary rf fields. The NMR signals were observed at the following frequencies: $\nu(^1H) = 90$ MHz, $\nu(^{19}F) = 84.6$ MHz, $\nu(^{13}C) = 22.6$ MHz, $\nu(^{109}Ag) = 4.2$ MHz.

Free-induction-decay signals were stored in a Datalab DL 905 transient recorder, averaged and Fourier transformed by a Varian 620 L on-line computer. The basic scheme for observing the weak signals of ^{13}C and ^{109}Ag under decoupling conditions was as follows:^{6,12}

(a) The abundant spins I (1H or ^{19}F) were "cooled" by adiabatic demagnetization in the ro-

TABLE I. Parameters used in the calculations for the two different spin systems $^{109}\text{Ag}-^{19}\text{F}$ in AgF and $^{13}\text{C}-^1\text{H}$ in adamantane ($\text{C}_{10}\text{H}_{16}$). The motion of the adamantane molecules at room temperature has been taken into account by a simple model.

Sample	AgF			Adamantane			$\text{C}_{10}\text{H}_{16}$	
γ_I	(^{19}F)	25 167	$\text{sec}^{-1}\text{G}^{-1}$	(^1H)	26 748	$\text{sec}^{-1}\text{G}^{-1}$		
γ_S	(^{109}Ag)	1 244	$\text{sec}^{-1}\text{G}^{-1}$	(^{13}C)	6 727	$\text{sec}^{-1}\text{G}^{-1}$		
a		2.46	\AA		4.725	\AA		
Direction of H_0	[100]	[110]	[111]	Powder average	[100]	[110]	[111]	Powder average
S_1	3.070	0.881	0.152	1.319	6.940	10.388	11.540	9.698
S_2	2.250	0.114	0.003	0.491	3.808	26.928	9.504	13.080
S_3	0.058	0.030	0.019	-0.012	9.580	7.457	15.219	7.528
S_4	0.820	0.337	0.063	0.444	43.876	80.464	123.054	81.912
$M_2^I S$ (rad/sec) ²	1.51×10^7	4.34×10^6	7.46×10^5	6.50×10^6	2.25×10^7	3.36×10^7	3.74×10^7	3.14×10^7
μ_1	2.52	2.71	2.75	2.64	2.84	2.50	2.86	2.73
μ_2	16.62	81.12	395.89	90.89	5.63	5.34	6.40	6.21
τ_{c0} (μsec)	89	75	82	74	126	106	91	102

tating frame (ADRF).

(b) Then a strong rf field $H_{1S} = \omega_{1S}/\gamma_S$ was applied at the resonance frequency of the S spins (whether ^{13}C or ^{109}Ag).

The operating mode was "unmatched" Hartman-Hahn condition ($\omega_{1S} \gg \omega_{LI}$) to achieve maximum polarization in one shot.^{7,24}

(c) After termination of H_{1S} a rf field H_{1I} of the order of 20 G was applied to the I spins and the free-induction decay of the S spins was observed.

Figure 7 gives a schematical representation of the pulse timing and the experimental setup. A review of the different techniques involved may be found in Ref. 12. It should be noted, that the silver resonance signal is very weak because of the small gyromagnetic ratio and many accumulations have been taken in order to observe the signal.

V. EXPERIMENTS AND DISCUSSION

Experimental spectra of ^{109}Ag in AgF and of ^{13}C in adamantane were taken as described in Sec. IV. The excess line shape $J(\omega)$ due to the I-S interaction was obtained by deconvolution of the observed spectra with the totally decoupled spectrum. The linewidth at half-height $\Delta\nu = \delta/\pi$ in hertz, where δ is the halfwidth in angular frequency units, was directly determined from the excess line shape. The parameters used for the theoretical calculations are summarized in Table I. Figure 8 gives a schematic representation of the (010) plane in the fcc unit cell together with the parameters used for the calculation of the lattice sums. In

the case of adamantane globular-shaped molecules have been assumed with radius $R = 3.34 \text{\AA}$, which are reorienting rapidly at room temperature. The average over this motion is taken into account by using^{14,25}

$$\langle r_{ij}^{-3} \rangle = r_{0ij}^{-3} (1 - \epsilon^2)^{-1},$$

with

$$\epsilon = R/r_{0ij}.$$

This implies a simple model for the motion by assuming the interaction between a point nucleus and nuclei distributed on the surface of a sphere. Although this may be a good enough approximation for the intermolecular $^{13}\text{C}-^1\text{H}$ interaction, it certainly is not valid for the internuclear proton interaction. However the theoretical results are not expected to change appreciably if a different model for the proton-proton interaction is assumed. Since the exact motion of the molecules is not known anyway, we leave this to a more detailed analysis.

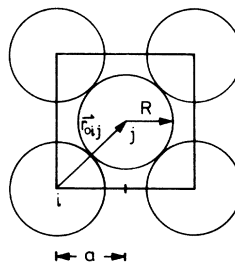


FIG. 8. (010) plane of the fcc unit cell with the lattice constant a . The necessary parameters for obtaining lattice sums are indicated.

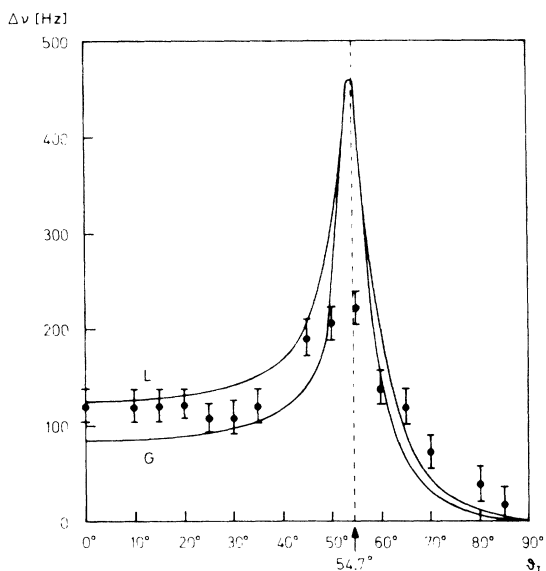


FIG. 9. Measured (points) and calculated (lines) ^{109}Ag resonance excess linewidth $\Delta\nu$ in an AgF powder sample versus ϑ_I . A real powder average has been performed in the calculation applying the mixed memory function approach as discussed in the text. L stands for Lorentzian and G for Gaussian memory function, respectively.

The calculations in the following have been performed using the parameters given in Table I. The orientation dependence of the lattice parameters has been computed for different cubic lattices, but will be presented elsewhere. Notice, that no adjustable parameter is used throughout the calculations and only the approximations as described in Sec. III are employed.

Figure 9 represents the experimental and theoretical linewidth $\Delta\nu$ of the ^{109}Ag signal in a AgF powder sample for different angles ϑ_I of the rf field in the I -spin rotating frame. The "natural", i.e., undecoupled linewidth is observed for $\vartheta_I=0$, whereas for $\vartheta_I=\frac{1}{2}\pi$ the linewidth vanishes, i.e., complete decoupling. A line broadening is seen to occur at the magic angle $\vartheta_I=54.7^\circ$. As discussed above, the linewidth at the magic angle can be calculated rigorously, leading to a value of $\Delta\nu=453$ Hz. The reason that the experimental data do not reach this value is believed to be due to rf inhomogeneity of the decoupling field. A crossed coil arrangement was used in the probehead which produced rf fields with poor homogeneity. This results in a large distribution of ϑ_I values, leading to a large contribution of the narrower lines from regions $\vartheta_I \neq 54.7^\circ$. This problem may be circumvented by applying appropriate multiple pulse cycles^{11,12,21} to the I spins to compensate to a certain extent

for rf inhomogeneity. An application of these techniques is currently under investigation. The calculated linewidth using the mixed memory function approach agrees with the rigorous linewidth at the magic angle as expected and shows quite a good agreement with the experimental data in the other regions of ϑ_I .

The Lorentzian assumption of $K_{II}(t)$ seems to represent the data more closely than the Gaussian assumption. Since the linewidth is strongly orientation dependent, a real powder average for the calculated line shape has been performed, i.e., for each orientation of the magnetic field H_0 the line shape was calculated using the mixed memory-function approach, from which the powder line shape was calculated by averaging over all orientations. The theoretical linewidth $\Delta\nu$ as plotted in Fig. 9 was then read of the calculated average line shape directly.

Figure 10 represents similar data as obtained for the ^{13}C linewidth in adamantane ($\text{C}_{10}\text{H}_{16}$) powder at room temperature. The rapid rotation of the globular-shaped molecules which form a fcc lattice

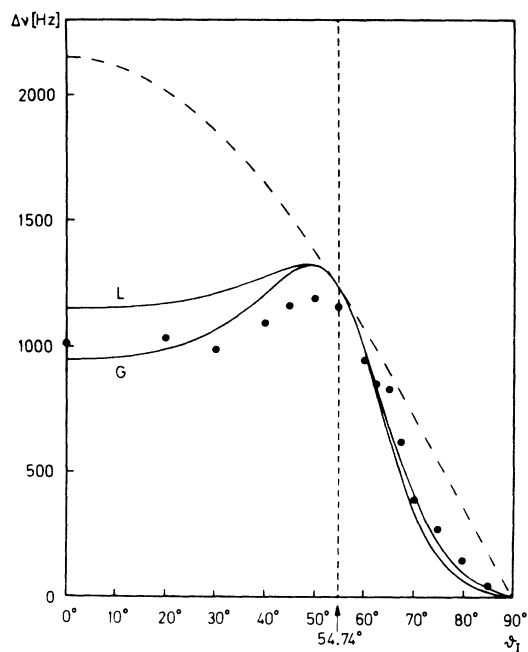


FIG. 10. Measured (points) and calculated (lines) ^{13}C resonance excess linewidth $\Delta\nu$ in adamantane ($\text{C}_{10}\text{H}_{16}$) powder vs the angle ϑ_I of the effective field in the ^1H rotating frame. A real powder average has been performed in the calculation applying the mixed memory-function approach as discussed in the text. The dashed line shows the expected linewidth variation if no I spin flip-flop motion would be present. (L: Lorentzian, G: Gaussian memory function, see text.)

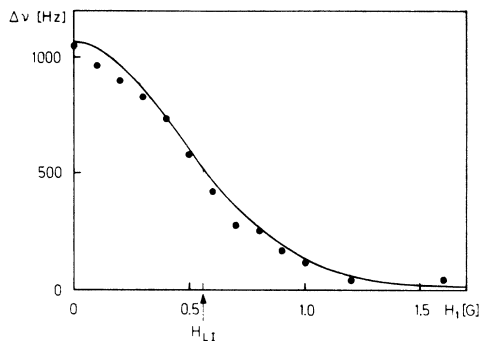


FIG. 11. Measured (points) and calculated (lines) ^{13}C resonance excess linewidth $\Delta\nu$ in adamantane ($\text{C}_{10}\text{H}_{16}$) powder versus the on-resonance decoupling field $H_{L1} = \omega_I/\gamma_I$ applied to the proton resonance. The theoretical line is obtained as explained in the text. (H_{L1} : local field of the protons.)

has been taken into account.¹⁴ The line broadening near the magic angle does not appear to be too dramatic since the ratio γ_I/γ_S is only about 4 instead of 20 as in the case of AgF. H_1 field inhomogeneity at the I -spin resonance does not affect the linewidth peaking at the magic angle therefore as drastically as in the case of AgF. In contrast to Ref. 14, a real powder average has been performed as discussed above in the calculation of the linewidth $\Delta\nu$ as represented in Fig. 10.

We ended the discussion about the efficiency of on-resonance decoupling in the case of dipolar coupling among many nuclear spins in the theoretical Sec. III case (C). The memory-function approach allows us to solve the problem in terms of calculating the S -spin resonance line shape and therefore the linewidth, by assuming a functional form for the

memory function. We have performed this calculation for adamantane powder by assuming a Gaussian memory function and using the time evolution operator $S_1(t)$ according to Eq. (85). The calculated linewidth $\Delta\nu$ is compared with the experimental data in Fig. 11. The agreement is quite good, although perhaps fortuitous. However, the qualitative behavior is not expected to change appreciably, when changing the functional form of the memory function as was demonstrated in the case of off-resonance decoupling. Note that the excess linewidth $\Delta\nu$ of the S -spin resonance is reduced to about its half value, when the rf field applied to the I spins equals the "local field" H_{LI} , which is defined by

$$\text{Tr}(3C_{II}^2) = \gamma_I^2 H_{LI}^2 \text{Tr}(I_z^2).$$

The "local field" of the I spins is therefore the critical value, which has to be overcome by the external rf field in order to produce appreciable decoupling between I and S spins. This however is true only if there is a coupling among many I spins. In I -spin pairs or triples, for example, multiple quantum transitions make the decoupling much more effective, as has been shown elsewhere.²⁶

ACKNOWLEDGMENTS

We gratefully acknowledge the continuous stimulating conversation we had on this subject with Professor A. Pines, who also carefully read the manuscript. We are indebted to Professor O. Kanert for interesting discussions. A considerable financial support of the Deutsche Forschungsgemeinschaft is gratefully appreciated.

¹(a) A. Abragam, *The Principles of Nuclear Magnetism* (Oxford U.P., London, 1961); (b) P. Mansfield, *Phys. Rev.* **137**, A961 (1965); (c) I. J. Lowe and R. E. Norberg, *Phys. Rev.* **107**, 46 (1957).

²A. Abragam and J. Winter, *C. R. Acad. Sci. (Paris)* **249**, 1633 (1959).

³F. Bloch, *Phys. Rev.* **111**, 841 (1958).

⁴L. R. Sarles and R. M. Cotts, *Phys. Rev.* **111**, 853 (1958).

⁵D. A. McArthur, E. L. Hahn, and R. E. Walstedt, *Phys. Rev.* **188**, 609 (1969).

⁶A. Pines, M. Gibby, and J. S. Waugh, (a) *J. Chem. Phys.* **56**, 1776 (1972); (b) **59**, 569 (1973).

⁷A. Pines and T. W. Shattuck, *J. Chem. Phys.* **61**, 1255 (1974).

⁸D. Demco, J. Tegenfeldt, and J. S. Waugh, *Phys. Rev. B* **11**, 4133 (1975).

⁹(a) Luciano Müller, Anil Kumar, Thomas Baumann, and Richard R. Ernst, *Phys. Rev. Lett.* **32**, 1409 (1974); (b) R. K. Hester, J. L. Ackermann, V. R.

Cross, and J. S. Waugh, *Phys. Rev. Lett.* **34**, 993 (1975); (c) J. S. Waugh, *Proc. Natl. Acad. Sci.* **73**, 5 (1976).

¹⁰(a) M. E. Stoll, W. K. Rhim, and R. W. Vaughan, *J. Chem. Phys.* **64**, 4808 (1976); (b) M. E. Stoll, A. J. Vega, and R. W. Vaughan, *ibid.* (to be published).

¹¹U. Haeblerlen, *Advances in Magnetic Resonance*, edited by J. S. Waugh, (Academic, New York, 1976).

¹²M. Mehring, *High Resolution NMR Spectroscopy in Solids, in NMR: Basic Principles and Progress* (Springer-Verlag, Heidelberg, 1976), Vol. 11.

¹³M. Mehring, G. Sinnig, and A. Pines, *Z. Phys. B* **24**, 73 (1976).

¹⁴G. Sinnig, M. Mehring, and A. Pines, *Chem. Phys. Lett.* **43**, 382 (1976).

¹⁵H. T. Stokes and D. C. Ailion (private communication).

¹⁶M. Lee and W. I. Goldberg, *Phys. Rev.* **140**, A1261 (1965).

¹⁷R. Zwanzig, *Lectures in Theoretical Physics* (Interscience, New York, 1961).

- ¹⁸F. Lado, J. D. Memory, and G. W. Parker, *Phys. Rev. B* 4, 1406 (1971).
- ¹⁹(a) H. Mori and K. Kawasaki, *Prog. Theor. Phys.* 27, 529 (1962); (b) H. Mori, *ibid.* 33, 423 (1965); 34, 399 (1965).
- ²⁰R. E. Walstedt, *Phys. Rev. B* 5, 41 (1972).
- ²¹U. Haerberlen and J. S. Waugh, *Phys. Rev.* 175, 453 (1968).
- ²²(a) M. Mehring, H. Raber, and G. Sinning, *Proceedings of the Eighteenth Congress Ampere, Nottingham, England, 1974* (Nottingham U. P., Nottingham, 1974), p. 35.
- ²³H. Bateman, *Higher Transcendental Functions* (McGraw-Hill, New York, 1953), Vol. II, p. 143.
- ²⁴A. Pines, Proceedings of the First Ampere Spectroscopy Colloquium, Krakow, Poland, 1973 (unpublished).
- ²⁵E. R. Andrew and R. G. Eades, *Proc. R. Soc. A* 216, 398 (1953).
- ²⁶(a) A. Pines, D. J. Ruben, S. Vega, and M. Mehring, *Phys. Rev. Lett.* 36, 110 (1976); (b) A. Pines, S. Vega, and M. Mehring (unpublished).